International Atomic Energy Agency

INDC(YUG)-7

Distr: G V

INDC INTERNATIONAL NUCLEAR DATA COMMITTEE

# CALCULATION OF MULTIGROUP CONSTANTS IN WIMS FORMAT WITH PROGRAMS FEDGROUP AND FLANGE AND COMPARISON OF THE RESULTS OBTAINED USING DIFFERENT EVALUATED LIBRARIES

A.Trkov, M.Budnar, M.Čopič, A.Perdan and M.Ravnik
J.Stefan Institute, E.Kardelj University of Ljubljana

univerza v ljubljani

institut "jožef stefan" ljubljana, jugoslavija

Jan. 1982

IAEA NUCLEAR DATA SECTION, WAGRAMERSTRASSE 5, A-1400 VIENNA

INDC(YUG)-7

(1185)

INDC(YUG)-7
Distr.: G V

# CALCULATION OF MULTIGROUP CONSTANTS IN WIMS FORMAT WITH PROGRAMS FEDGROUP AND FLANGE AND COMPARISON OF THE RESULTS OBTAINED USING DIFFERENT EVALUATED LIBRARIES

A. Trkov, M. Budnar, M. Čopič, A. Perdan and M. Ravnik
J. Stefan Institute, E. Kardelj University of Ljubljana

Univerza v Ljubljani
INSTITUT "JOŽEF STEFAN" LJUBLJANA, JUGOSLAVIJA

Jan. 1982

Reproduced by IAEA, July 1982

# CALCULATION OF MULTIGROUP CONSTANTS IN WIMS FORMAT WITH PROGRAMS FEDGROUP AND FLANGE AND COMPARISON OF THE RESULTS OBTAINED USING DIFFERENT EVALUATED LIBRARIES

A.Trkov, M.Budnar, M.Čopič, A.Perdan and M.Ravnik
J.Stefan Institute, E.Kardelj University of Ljubljana

Abstract

Multigroup constants for 1-H-1, 92-U-235, 92-U-238 have been calculated. Averaged cross-sections and other constants have been prepared in the WIMS 69-group format. Comparison has been made between group constants obtained with several evaluated libraries (KEDAK-3 1975, 1979, ENDF/B-4, ENDF/B-5) and the WIMS-D library. Observed differences are most pronounced in the resonance and fast region. From test runs on fuel cell with WIMS program it can be deduced that these differences affect the fewgroup constants significantly.

## 1. Introduction

In connection with the PWR power plant built at Krško, Jugoslavia, there has been noted and increased interest in the Light Water Reactor analysis, especially in the areas of lattice calculations as a basis for global reactor analysis including burnup.

The CDC version of the code WIMS has been available recently[13] and is now widely used in the thermal reactor calculations for few group constants preparation. The input library for the package is based on UKNDL (1968) evaluated nuclear data library and corrected on the basis of integral experiments. Our aim was to investigate the possibility of creating a multigroup data library directly from the evaluated nuclear data files and compare them with the WIMS input library. This would enable us to produce independent analysis of the reactor parameters and the design specifications. It would also give an insight into the dependence of the reactor parameters on the multigroup data, with the possibility to extend and improve the basic multigroup library. The choice of the programs used in the calculations was governed by the fact that not all recent evaluated data libraries were available to us and that the calculations were to be performed on the CDC-Cyber 72 machine which imposes a rather severe memory requirement on the programs.

The multigroup constants were calculated with the corrected version of the multigroup code FEDGROUP[9,10]. In the thermal region the CDC version of the code FLANGE-AE[11,12] was used. We examined the differences between multigroup constants obtained from several evaluated data libraries and their effects on few-group constants. For the purpose of analysis the data from KEDAK-3 (1975)[2], KEDAK-3 (1979)[3] ENDF/B-4[4,5], ENDF/B-5[6,7] and WIMS-D[8] were considered. Note that for U-238 ENDF/B-5 calculations only the radiative capture and the fission

cross-section are taken from the ENDF/B-5 file. The rest are available only in the ENDF/B-4 version but these data however are only of secondary importance.

## 2. Multigroup Constants for Preparing The WIMS Library

The program system FEDGROUP is able to calculate group averaged constants for reactor calculations from various evaluated data files disseminated by IAEA (ENDF/B, KEDAK, UKNDL formats). The averaging can be done in an arbitrary group structure and using an arbitrary averaging spectre. The data can be given pointwise or by resolved and unresolved resonance parameters for the Single-level or the Multilevel Breit-Wigner formula, taking Doppler broadening into account. They are processed to infinite dilute and resonance screened group averaged cross-sections. Elastic and inelastic scattering matrices can also be calculated from the angular distributions of secondary neutrons and from scattering into resolved and unresolved excitation levels, respectively, as well as the Greuling-Goertzel constants, if required.

In the thermal region the scattering matrix is calculated by the program package FLANGE either from the ENDF/B scattering law data (since no other evaluated data file contains differential thermal scattering data) or from a simulated input file in ENDF/B format to effect the free-gas or the difussion model for the scattering matrix calculation. The results of FLANGE are then converted into FEDGROUP format by an auxilliary program FLACOF[10].

The constants are calculated in 69 group system as defined in Table 1. The 69 group structure is identical to the one in the WIMS input library, and is adequate for the thermal reactor cell calculations. The energy groups in the fast and the resonance region are relatively wide. Fine group structure is used

in the epithermal region to cover the first U and Pu resonances which essentially influence the shape of the neutron spectre in the cell calculations. For the cell and the global reactor analysis performed on the basis of the created 69 group libraries further condensation to 18 group and 2 group structure is performed using the S-WIMS code.

The averageing spectre for the multigroup constants calculations was the Maxwell-Boltzman distribution up to 0.1 eV, the 1/E spectre up to 67 KeV and the Watt fission spectre above 67 keV.

The above mentioned FEDGROUP and FLANGE results were processed by the code FEDWIM[10] so that complete data sets (table 6) for a specified material were introduced into the WIMS data library under a new nucleide identification number. The structure of the library[8] remained unchanged and the old data accessible.

## 3. Comparison of the Multigroup Constants from Various Evaluated Data Libraries

For simplicity the comparison has been limited to the most delicate reaction types of the most important thermal reactor materials. These are considered to be the fission yield of U-235, absorption of U-238 and scatter on hydrogen bound in water. Plutonium isotopes with mass 239 and 241 had also been calculated but since they only affect the reactor core when burn-up proceeds, they had been excluded from the present analysis.

### 3.1. U-235

From Fig. 1 it can be seen that in the period 1975-1979 in the KEDAK-3 library there were no major changes in the fission yield of U-235 in the fast region and the region of unresolved reso-

nances. There is a marked decrease in the resonance region especially around the 1.1. resonance where the new absorption data are up to 26 % lower than either the 1975 evaluation, the ENDF/B data (Fig. 3) or the WIMS data (Fig. 4). Any spurious error on the file is excluded because the cross-sections in this region are consistent when calculated either from resonance parametersor from pointwise data.

The differences between the ENDF/B-4 to ENDF/B-5 data are small (Fig. 2, table 5). In the resonance and the fast region the agreement between WIMS and ENDF/B group data is good (Fig. 5). Nevertheless the WIMS data are slightly higher in the resolved resonance region while in the unresolved region the situation is reversed. The discrepancies have no significant effect on the non-thermal part of the spectre nor on the effective 2-group constants as can be seen from Table 3. This is not the case for KEDAK data. Below about 3 eV the agreement between all data is good (less than 7 % difference and decreasing with energy) except for KEDAK-3 (1979) as already noted before.

The differences in the resonance screened tabulations closely follow the trends of the data at infinite dilution so they had not been analysed separately.

### 3.2. 92-U-238

Comparing infinite dilute multigroup cross sections it can be seen that the absorption cross section of U-238 on KEDAK-3 (1979) file is consistently lower by a few percent than the older evaluation (Fig. 6). The agreement between the KEDAK-3 (1979) and ENDF/B-5 evaluations (Fig. 8) is thus quite good (less than 5 % difference in the fast and thermal region and about 10 % in the resolved resonance region) except in a few energy groups in the region of unresolved resonances (in group 16 the difference reaches 30 % relative to ENDF/B-V).

It is to be emphasized at this stage that we can not expect the calculated group averaged cross sections to agree with the data in WIMS-D library in the resonance region since these data were adjusted artificially to give good results for the benchmark problems considered (Fig. 9, 10). The resonance absorption cross section data for U-238 as they are in the WIMS 69-group library are significantly smaller compared to ENDF/B-5 or KEDAK results. In cell calculations as a consequence the epithermal and fast parts of the neutron spectra calculated from ENDF/B-5 data tend to be smaller than when calculated on the basis of the original WIMS-D library (Table 3).

In the case where U-238 appears in large concentrations resonance screening effects are very important. The dependence of the resonance screened data on the background cross section can be seen in Table 2. Data are presented at 900 K and at several concentrations given in terms of the background cross section ($\sigma_o$) defined as the macroscopic effective potential cross section of the mixture of materials per absorber nucleus taking composition and geometry into account. As the differences in the infinite dilute cross sections between KEDAK-3 (1979) and ENDF/B-5 libraries are not so large (Fig. 8) it is evident that the width of the resonances contributes to the discrepancies. KEDAK-3 (1979) resonance screened absorption cross-sections decrease faster with increasing concentration than the corresponding values calculated from the ENDF/B-files. As seen from Table 2 there had been some modifications in the ENDF/B-5 evaluation as compared to the verison 4 however the most significant changes can be found in the groups 24 to 27 which contain the first three s-wave resonances. A considerable decrease in the resonance screened absorption cross-section can be observed what agrees well with the reduction in the capture width of the above mentioned resonances as reported in (6) relative to ENDF/B-4 evaluation.

No resonance screened data are presented for KEDAK-3 (1975) since the resonance parameters from which more accurate resonance screened data can be obtained, are not recommended for calculations by the KEDAK evaluators.

3.3. 1-H-1

KEDAK - library contains no thermal scattering data so the calculations were performed only from the ENDF/B file which remained unaltered since the version ENDF/B-3[5] was issued and is still recommended for use.

The only observable differences between the scattering cross sections in WIMS-D and ENDF/B files are in the thermal region (Fig. 11). The differences can be accounted for by the fact that the Haywood model is used in the ENDF/B evaluation and the effective width model in the WIMS-D evaluation. The former produces somewhat harder neutron spectre in the thermal region what may affect the results of the reactor calculations.

In calculating the transport cross-section according to the standard formulae we noticed a considerable discrepancy in the fast region between the values calculated from ENDF/B and the WIMS-D library values. To avoid errors the $P_1$ matrix was used by choosing the option which solves the transport equation in the $B_1$ approximation in the fuel cell calculation.

## 4. Verification of the results through cell and criticality calculations and comparison with experiment

The 69-group data libraries obtained on the basis of KEDAK-3, ENDF/B-4 and ENDF/B-5 were used in all calculations performed with the use of the programme S-WIMS. Results were compared to those obtained with the original WIMS library and are summarized in Table 3. The unit cell is of the PWR type (Krško, NPP, ref. 1) at operating conditions of zero power.

The global reactor calculation of two group neutron flux and criticality was performed for the same reactor core and the same conditions, on the basis of cell calculations performed by WIMS program from the original 69 WIMS input library and the

one ammended by the ENDF/B-5 data. The results were compared with design and experimental values. The results on the basis of both data libraries are in good agreement with design calculations and experimental values, as can be seen from Table 4 and Fig 12. The results calculated by WIMS on the basis of the original data library, being in excellent agreement with design calculations and measurements, were taken as a reference for comparison with the results obtained with other data libraries.

The effects arising from the differences between the data libraries can be traced throughout the entire procedure of the cell calculations and group condensation and are observable in two group diffusion parameters (Table 3). The most remarkable effects arise from the differences in $\sigma_a$ of U-238 in the fast, the resonance and the epithermal region. The fast absorption cross section calculated from ENDF/B is higher then that from the WIMS library. The consequence is the reduction of the fast spectre which also influences the fast group constants. Higher absorption of the low energy U-238 resonances reduces the epithermal and even the thermal part of the spectre. Further reduction of the epithermal and thermal spectre is caused by relatively high $\sigma_a$ of U-235 in the thermal region for the case of ENDF/B-5 data as can be seen from Table 5. The overall result is that for a thermal reactor the whole energy scale spectre beeomes harder for ENDF/B-5 data.

The consequence is observable in reduced $k_\infty$ for a typical unit fuel cell (Table 3) as well as in $k_{eff}$ from the global reactor criticality calculations (Table 4). The reduction of $k_{eff}$ for about 100 pcm is caused mainly by an increased fast neutron leakage and partly by the higher effective thermal microscopis absorption cross section which are both sensitive to the harder neutron spectre.

The influence of the hardened neutron spectre is also noticed on the unit cell and fuel element disadvantage factors. It can be seen from Fig. 12 that the spatial thermal flux distribution undergoes about 2 % smaller variations between the regions of different material composition for BNDF/B-5 data as a consequence of the increased fast leakage from the unit cell and the fuel element.

## 5. Conclusion

From the cell and the global reactor calculations it can be deduced that the differences between the original WIMS and the ENDF/B-5 library lead to certain differences in the core reactivity and flux distributions. Nevertheless they are minimal and within tolerance for all reactor calculations. From the reactor analysis point of view it can be concluded that the evaluated few group nuclear data calculated from ENDF/B-5 with the use of the programmes FEDGROUP-C and FLANGE-AE form a complete and reliable set of data for thermal reactor calculations. Furthermore they can compete with the data corrected through the integral reactor experiments such as the original WIMS data library.

References

1. Krško NPP Final Safety Analysis Report, Westinghouse 1978

2. Status of Nuclear Data Library KEDAK-3 October 1975
KFK 2234, NEANDC(E) 171 "U"

3. KEDAK-3 Version of Feb. 1979

4. ENDF/B-4 data files for

| Material | Mat. | Author | Institution |
|---|---|---|---|
| 91-U-235 | 1261 | L.Stewart | LASL |
| | | A.Alter | AI |
| | | R.Hunter | LASL |
| 92-U-238 | 1262 | N.C.Paik | WARD |
| 1-H-1 | 1269 | L.Stewart | LASL |
| | (MOD 2) | R.J.Labauve | LASL |
| | | P.G.Young | LSL |

BNL-NCS-17541 (ENDF-201) 2 Edition, D.Garber (Oct. 1975)
Brookhaven National Laboratory, Upton N.Y.

5. ENDF/B-3 scattering law data for material 1-H-1 bound in $H_2O$, (MAT1002) evaluated at Brookhaven National laboratory using code GASKET

6. ENDF/B-5 standards data file for material 92-U-235 (MAT 1395, MOD 1) evaluation by M.R.Bhat

BNL-NCS-17541 (ENDF-201) 3rd Edition (July 1979), R.Kinsley
Brookhaven National Laboratory, Upton N.Y.

7. ENDF/B-5 dosimetry files, material 92-U-238
(MAT 6398, MOD 1)

BNL-NCS-17541 (ENDF-201) 3rd Edition (July 1979), R.Kinsley
Brookhaven National Laboratory, Upton, N.Y.

8. The WIMS 69 Group Library
C.J.Taubman, AAEW-MI324 July 1975

9. FEDGROUP-A program system for producing group constants from evaluated nuclear data of files disseminated by IAEA P.Vertes, INDC (HUN)-13/L+Sp (1976) and INDC(HUN)-15/L (1979)

10. FEDGROUP-C A CDC version of the modifies FEDGROUP program for evaluating group constants from data libraries in ENDF/B, KEDAK and UKNDL formats A.Trkov, A.Perdan, M.Budnar, Institute J.Stefan, Ljubljana, Yugoslavia, to be published.

11. FLANGE II Version 71-1 A code to process thermal neutron data from an ENDF/B tape, H.C.Honech and D.R.Finch, Du Pont, Savannah River Lab. Aiken South Carolina, DP-1278, ENDF-152, 1971

12. K.Nyman, FLANGE-AE, NEA-CPL, Saclay

13. I.R.Askew, F.I.Fayers, P.B.Kemsharle, A General Description of the Lattice code WIMS, JBNES 564 (1968)

14. K.Kowalska, The S-WIMS code for the CYBER 72 Computer, NEA-CPL, Saclay

15. Nuclear Data Needs for LWR Applicaations, Odelli Ozer, Proceedings of the International Conference on Nuclear Cross Sections for Technology, Knoxville, Tennessee Oct. 1979

Table 1: 69-group structure of WIMS input data library together with 18-group and 2-group structure for transport cell and global reactor calculations respectively

| 2-group fast | | | 2-group thermal | | |
|---|---|---|---|---|---|
| 69 gr. | 18 gr. | Upper energy bound (eV) | 69 gr. | 18 gr. | Upper energy bound (eV) |
| 1 | 1 | 10 000 000. | 37 | 10 | 1.071 |
| 2 | | 6 065 000. | 38 | | 1.045 |
| 3 | 2 | 3 679 000. | 39 | | 1.020 |
| 4 | | 2 231 000. | 40 | 11 | 0.996 |
| 5 | | 1 353 000. | 41 | | 0.972 |
| 6 | 3 | 821 000. | 42 | | 0.95 |
| 7 | | 500 000. | 43 | | 0.91 |
| 8 | | 302.000. | 44 | | 0.85 |
| 9 | | 183 000. | 45 | | 0.78 |
| 10 | | 111 000. | 46 | 12 | 0.625 |
| 11 | 4 | 67 340. | 47 | | 0.5 |
| 12 | | 40 850. | 48 | | 0.4 |
| 13 | | 24 780. | 49 | 13 | 0.35 |
| 14 | | 15 030. | 50 | | 0.32 |
| 15 | | 9 118. | 51 | | 0.3 |
| 16 | 5 | 5 530. | 52 | | 0.28 |
| 17 | | 3 519.1 | 53 | | 0.25 |
| 18 | | 2 239.45 | 54 | 14 | 0.22 |
| 19 | | 1 425.1 | 55 | | 0.18 |
| 20 | | 906.898 | 56 | | 0.14 |
| 21 | | 367.262 | 57 | 15 | 0.1 |
| 22 | | 148.728 | 58 | | 0.08 |
| 23 | | 75.5014 | 59 | | 0.067 |
| 24 | 6 | 48.052 | 60 | | 0.058 |
| 25 | 7 | 27.7 | 61 | 16 | 0.05 |
| 26 | | 15.968 | 62 | | 0.042 |
| 27 | 8 | 9.877 | 63 | | 0.035 |
| 28 | 9 | 4.0 | 64 | 17 | 0.03 |
| 29 | | 3.3 | 65 | | 0.025 |
| 30 | | 2.6 | 66 | 18 | 0.02 |
| 31 | | 2.1 | 67 | | 0.015 |
| 32 | | 1.5 | 68 | | 0.01 |
| 33 | | 1.3 | 69 | | 0.005 |
| 34 | | 1.15 | | | |
| 35 | | 1.123 | | | |
| 36 | | 1.097 | | | |

Table 2: Absorption resonance tables for U-238 at 900 K (cros sections in barns)

| Gr | $\sigma_o$ | WIMS-D | ENDF/B-4 | ENDF/B-5 | KEDAK-3 |
|---|---|---|---|---|---|
| 15 | 15.5 | .6655 | .7909 | .8056 | .7856 |
| | 65.3 | .7704 | .8467 | .8623 | .8226 |
| | 1000. | .8482 | .8944 | .9100 | .8483 |
| 16 | 15.5 | .8201 | .8232 | .8246 | .4760 |
| | 65.3 | .9873 | .9155 | .9202 | .5371 |
| | 1000. | 1.119 | 1.062 | 1.07 | .7037 |
| 17 | 15.5 | .3979 | .8240 | .8483 | .6178 |
| | 65.3 | .5881 | .9229 | .9618 | .7149 |
| | 1000. | .7998 | 1.278 | 1.341 | 1.056 |
| 18 | 15.5 | .6264 | .8114 | .8054 | .5740 |
| | 65.3 | 1.041 | .9553 | .9682 | .7290 |
| | 1000. | 1.638 | 1.520 | 1.551 | 1.281 |
| 19 | 15.5 | .6356 | .9658 | .9229 | .9089 |
| | 65.3 | 1.114 | 1.190 | 1.189 | 1.150 |
| | 1000. | 2.005 | 2.143 | 2.211 | 2.152 |
| 20 | 15.5 | .7594 | 1.073 | 1.073 | 1.003 |
| | 65.3 | 1.387 | 1.472 | 1.486 | 1.385 |
| | 1000. | 2.695 | 2.886 | 2.885 | 2.704 |
| 21 | 15.5 | .8542 | 1.047 | 1.038 | .9811 |
| | 65.3 | 1.769 | 1.794 | 1.790 | 1.702 |
| | 1000. | 5.344 | 5.781 | 5.641 | 5.484 |
| 22 | 15.5 | 1.378 | 1.587 | 1.548 | 1.543 |
| | 65.3 | 2.826 | 2.953 | 2.885 | 2.870 |
| | 1000. | 9.337 | 11.13 | 10.81 | 10.93 |
| 23 | 15.5 | 1.064 | 1.223 | 1.245 | 1.194 |
| | 65.3 | 2.487 | 2.531 | 2.576 | 2.486 |
| | 1000. | 11.63 | 12.79 | 12.82 | 12.62 |
| 24 | 15.5 | 2.289 | 2.470 | 2.412 | 2.446 |
| | 65.3 | 5.070 | 5.064 | 4.961 | 4.954 |
| | 1000. | 23.052 | 26.24 | 25.72 | 25.90 |
| 25 | 15.5 | 2.698 | 3.270 | 3.231 | 3.386 |
| | 65.3 | 6.491 | 6.770 | 6.742 | 6.651 |
| | 1000. | 35.168 | 36.67 | 37.18 | 37.15 |
| 26 | 15.5 | .1980 | .4775 | .5003 | .4661 |
| | 65.3 | .2070 | .4445 | .4681 | .4259 |
| | 1000. | .2100 | .4549 | .4748 | .4648 |
| 27 | 15.5 | 3.554 | 4.334 | 4.158 | 4.573 |
| | 65.3 | 8.445 | 8.822 | 8.434 | 8.330 |
| | 1000. | 44.75 | 45.23 | 44.31 | 44.60 |

Tabela 3: Comparison of the macroscopic cell-homogenised group constants calculated for the fuel cell using data from different evaluated libraries.

| | gr | WIMS-D | ENDF/B-4$ | ENDF/B-4* | ENDF/B-5$ | KEDAK-3$ |
|---|---|---|---|---|---|---|
| k | | 1.11662 | 1.10496 | 1.10688 | 1.11629 | 1.10609 |
| diff. coeff. | 1 | 1.3297E 0 | 1.3369E 0 | 1.3484E 0 | 1.3384E 0 | 1.3543E 0 |
| | 2 | 4.5915E-1 | 4.5519E-1 | 4.6731E-1 | 4.5523E-1 | 4.5574E-1 |
| absorpt. $_a$($cm^{-1}$) | 1 | 1.0026E-2 | 1.0291E-2 | 1.0229E-2 | 1.0185E-2 | 0.9940E-2 |
| | 2 | 8.3119E-2 | 8.3787E-2 | 8.2774E-2 | 8.3630E-2 | 8.2893E-2 |
| removal $_{1-2}$($cm^{-1}$)2 | 1 | 1.4909E-2 | 1.4793E-2 | 1.4878E-2 | 1.4833E-2 | 1.4877E-2 |
| eff.fiss. $_f$($cm^{-1}$) | 1 | 6.3731E-3 | 6.3716E-3 | 6.3379E-3 | 6.3853E-3 | 6.0721E-3 |
| | 2 | 1.2024E-1 | 1.2111E-1 | 1.1957E-1 | 1.2167E-1 | 1.1933E-1 |
| flux(inf)1 ($cm^{-2}$) | 1 | 5.3932E14 | 5.3916E14 | 5.3581E14 | 5.3760E14 | 5.4199E14 |
| | 2 | 9.5767E13 | 9.3961E13 | 9.5560E13 | 9.4645E13 | 9.6545E13 |

$ WIMS-D data with the multigroup constants for U-235 and U-238 replaced by the group constants from the stated evaluated data library

* WIMS-D DATA WITH THE MULTIGROUP CONSTANTS FOR U-235, U-238 and H-1 replaced by the group constants calculated from the stated evaluated data library

Table 4: Comparison of the $k_{eff}$ for the global reactor criticality calculations of the Krško NPP core from different source data, for HZP conditions.

| $k_{eff}$ | source data |
|---|---|
| 1.00192 | WIMS-D original data |
| 1.00286 | WIMS-D data with the multigroup constants for U-235, U-238 and H- 1 replaced by the group constants calculated from ENDF/B-5 data |
| 1.00145 | WIMS-D data with the multigroup constants for U-235, U-238 replaced by the group constants calculated from ENDF/B-5 data. |

Note: Measured $k_{eff}$ for the same configuration and same operating conditions was approx. 1.00350

Table 5: Comparison of the absorption group constants for U-235 from various evaluated data libraries

| GR | WIMS-D (barns) | ENDF/B-4 (barns) | rel.dev. % | KEDAK-3 (barns) | rel.dev. % | ENDF/B-5 (barns) | rel.dev. % |
|---|---|---|---|---|---|---|---|
| 1 | 1.247E+00 | 1.796E+00 | 4.402E+01 | 1.523E+00 | 2.213E+01 | 1.931E+00 | 2.273E+01 |
| 2 | 1.197E+00 | 1.151E+00 | -3.818E+00 | 1.138E+00 | -4.888E+00 | 1.127E+00 | -5.801E+00 |
| 3 | 1.298E+00 | 1.280E+00 | -1.388E+00 | 1.291E+00 | -5.017E-01 | 1.272E+00 | -1.966E+00 |
| 4 | 1.342E+00 | 1.327E+00 | -1.101E+00 | 1.351E+00 | 6.423E-01 | 1.339E+00 | -2.220E-01 |
| 5 | 1.354E+00 | 1.334E+00 | -1.444E+00 | 1.333E+00 | -1.584E+00 | 1.313E+00 | -3.061E+00 |
| 6 | 1.371E+00 | 1.292E+00 | -5.740E+00 | 1.305E+00 | -4.813E+00 | 1.292E+00 | -5.711E+00 |
| 7 | 1.543E+00 | 1.413E+00 | -8.447E+00 | 1.418E+00 | -8.138E+00 | 1.409E+00 | -8.719E+00 |
| 8 | 1.716E+00 | 1.591E+00 | -7.271E+00 | 1.605E+00 | -6.499E+00 | 1.593E+00 | -7.177E+00 |
| 9 | 1.980E+00 | 1.826E+00 | -7.765E+00 | 1.887E+00 | -4.713E+00 | 1.825E+00 | -7.817E+00 |
| 10 | 2.371E+00 | 2.102E+00 | -1.136E+01 | 2.223E+00 | -6.273E+00 | 2.067E+00 | -1.285E+01 |
| 11 | 2.802E+00 | 2.439E+00 | -1.296E+01 | 2.615E+00 | -6.653E+00 | 2.385E+00 | -1.487E+01 |
| 12 | 3.208E+00 | 2.757E+00 | -1.405E+01 | 2.967E+00 | -7.525E+00 | 2.704E+00 | -1.570E+01 |
| 13 | 3.623E+00 | 2.457E+00 | -3.217E+01 | 3.107E+00 | -1.424E+01 | 2.985E+00 | -1.760E+01 |
| 14 | 4.288E+00 | 3.311E+00 | -2.280E+01 | 3.813E+00 | -1.109E+01 | 3.622E+00 | -1.554E+01 |
| 15 | 4.890E+00 | 4.236E+00 | -1.337E+01 | 4.528E+00 | -7.409E+00 | 4.551E+00 | -6.933E+00 |
| 16 | 5.771E+00 | 5.481E+00 | -5.025E+00 | 5.772E+00 | 1.040E-02 | 5.704E+00 | -1.161E+00 |
| 17 | 7.375E+00 | 6.573E+00 | -1.087E+01 | 6.921E+00 | -6.153E+00 | 6.826E+00 | -7.444E+00 |
| 18 | 9.052E+00 | 9.293E+00 | 2.662E+00 | 9.351E+00 | 3.298E+00 | 8.937E+00 | -1.270E+00 |
| 19 | 1.145E+01 | 1.333E+01 | 1.639E+01 | 1.267E+01 | 1.063E+01 | 1.339E+01 | 1.698E+01 |
| 20 | 1.609E+01 | 1.721E+01 | 6.955E+00 | 1.753E+01 | 8.925E+00 | 1.630E+01 | 1.305E+00 |
| 21 | 2.307E+01 | 2.981E+01 | 2.923E+01 | 2.851E+01 | 2.358E+01 | 2.804E+01 | 2.154E+01 |
| 22 | 3.750E+01 | 3.549E+01 | -5.373E+00 | 3.492E+01 | -6.885E+00 | 3.569E+01 | -4.840E+00 |
| 23 | 4.316E+01 | 5.979E+01 | 3.853E+01 | 5.944E+01 | 3.771E+01 | 5.979E+01 | 3.853E+01 |
| 24 | 7.498E+01 | 7.092E+01 | -5.409E+00 | 6.973E+01 | -7.006E+00 | 7.092E+01 | -5.409E+00 |
| 25 | 9.051E+01 | 8.752E+01 | -3.308E+00 | 8.789E+01 | -2.897E+00 | 8.752E+01 | -3.308E+00 |
| 26 | 8.763E+01 | 8.379E+01 | -4.377E+00 | 7.794E+01 | -1.106E+01 | 8.379E+01 | -4.377E+00 |
| 27 | 7.943E+01 | 7.319E+01 | -7.861E+00 | 7.240E+01 | -8.852E+00 | 7.319E+01 | -7.861E+00 |
| 28 | 4.365E+01 | 4.297E+01 | -1.558E+00 | 4.423E+01 | 1.338E+00 | 4.297E+01 | -1.558E+00 |
| 29 | 3.110E+01 | 2.969E+01 | -4.560E+00 | 3.184E+01 | 2.374E+00 | 2.969E+01 | -4.560E+00 |
| 30 | 1.468E+01 | 1.371E+01 | -6.602E+00 | 1.088E+01 | -2.594E+01 | 1.371E+01 | -6.602E+00 |
| 31 | 2.711E+01 | 2.662E+01 | -1.805E+00 | 2.385E+01 | -1.204E+01 | 2.662E+01 | -1.805E+00 |
| 32 | 2.481E+01 | 2.406E+01 | -3.028E+00 | 2.845E+01 | 1.464E+01 | 2.406E+01 | -3.028E+00 |
| 33 | 7.147E+01 | 6.842E+01 | -4.265E+00 | 8.340E+01 | 1.669E+01 | 6.842E+01 | -4.265E+00 |
| 34 | 1.413E+02 | 1.428E+02 | 1.020E+00 | 1.383E+02 | -2.188E+00 | 1.428E+02 | 1.020E+00 |
| 35 | 1.377E+02 | 1.379E+02 | 8.858E-02 | 1.277E+02 | -7.313E+00 | 1.379E+02 | 8.858E-02 |
| 36 | 1.205E+02 | 1.206E+02 | 7.052E-02 | 1.078E+02 | -1.057E+01 | 1.206E+02 | 7.052E-02 |
| 37 | 1.030E+02 | 1.020E+02 | -9.790E-01 | 9.860E+01 | -1.395E+01 | 1.020E+02 | -9.790E-01 |
| 38 | 9.001E+01 | 8.848E+01 | -1.697E+00 | 7.354E+01 | -1.830E+01 | 8.848E+01 | -1.697E+00 |
| 39 | 8.087E+01 | 7.997E+01 | -1.120E+00 | 6.378E+01 | -2.113E+01 | 7.997E+01 | -1.114E+00 |
| 40 | 7.467E+01 | 7.409E+01 | -7.778E-01 | 5.691E+01 | -2.379E+01 | 7.414E+01 | -7.149E-01 |
| 41 | 7.026E+01 | 7.036E+01 | 1.376E-01 | 5.240E+01 | -2.542E+01 | 7.004E+01 | -3.221E-01 |
| 42 | 6.637E+01 | 6.653E+01 | 2.325E-01 | 4.873E+01 | -2.659E+01 | 6.634E+01 | -5.529E-02 |
| 43 | 6.259E+01 | 6.283E+01 | 3.823E-01 | 4.595E+01 | -2.658E+01 | 6.285E+01 | 4.175E-01 |
| 44 | 6.074E+01 | 6.159E+01 | 1.390E+00 | 4.574E+01 | -2.470E+01 | 6.145E+01 | 1.172E+00 |
| 45 | 6.439E+01 | 6.621E+01 | 2.822E+00 | 5.124E+01 | -2.043E+01 | 6.593E+01 | 2.384E+00 |
| 46 | 7.927E+01 | 8.120E+01 | 2.430E+00 | 6.576E+01 | -1.705E+01 | 8.156E+01 | 2.868E+00 |
| 47 | 1.115E+02 | 1.110E+02 | -4.331E-01 | 8.936E+01 | -1.987E+01 | 1.119E+02 | 3.560E-01 |
| 48 | 1.562E+02 | 1.556E+02 | -3.854E-01 | 1.220E+02 | -2.189E+01 | 1.571E+02 | 5.832E-01 |
| 49 | 1.982E+02 | 1.976E+02 | -3.178E-01 | 1.575E+02 | -2.054E+01 | 1.997E+02 | 7.295E-01 |
| 50 | 2.263E+02 | 2.291E+02 | 1.226E+00 | 1.910E+02 | -1.558E+01 | 2.289E+02 | 7.535E-01 |
| 51 | 2.407E+02 | 2.420E+02 | 5.464E-01 | 2.195E+02 | -8.800E+00 | 2.413E+02 | 2.580E-01 |
| 52 | 2.370E+02 | 2.382E+02 | 5.364E-01 | 2.385E+02 | 6.613E-01 | 2.387E+02 | 7.470E-01 |
| 53 | 2.229E+02 | 2.251E+02 | 9.572E-01 | 2.334E+02 | 4.672E+00 | 2.234E+02 | 2.157E-01 |
| 54 | 2.148E+02 | 2.182E+02 | 1.585E+00 | 2.251E+02 | 4.760E+00 | 2.153E+02 | 1.932E-01 |
| 55 | 2.265E+02 | 2.304E+02 | 1.729E+00 | 2.370E+02 | 4.650E+00 | 2.279E+02 | 6.314E-01 |
| 56 | 2.646E+02 | 2.691E+02 | 1.725E+00 | 2.747E+02 | 3.820E+00 | 2.675E+02 | 1.096E+00 |
| 57 | 3.159E+02 | 3.200E+02 | 1.300E+00 | 3.253E+02 | 2.979E+00 | 3.189E+02 | 9.805E-01 |
| 58 | 3.584E+02 | 3.618E+02 | 9.321E-01 | 3.669E+02 | 2.352E+00 | 3.614E+02 | 8.158E-01 |
| 59 | 3.968E+02 | 4.000E+02 | 8.260E-01 | 4.013E+02 | 1.147E+00 | 3.995E+02 | 6.838E-01 |
| 60 | 4.347E+02 | 4.381E+02 | 7.699E-01 | 4.371E+02 | 5.318E-01 | 4.374E+02 | 6.015E-01 |
| 61 | 4.798E+02 | 4.833E+02 | 7.345E-01 | 4.807E+02 | 1.955E-01 | 4.824E+02 | 5.546E-01 |
| 62 | 5.340E+02 | 5.373E+02 | 6.063E-01 | 5.297E+02 | -8.145E-01 | 5.364E+02 | 4.505E-01 |
| 63 | 5.897E+02 | 5.927E+02 | 5.118E-01 | 5.809E+02 | -1.479E+00 | 5.919E+02 | 3.738E-01 |
| 64 | 6.495E+02 | 6.524E+02 | 4.383E-01 | 6.374E+02 | -1.867E+00 | 6.515E+02 | 3.018E-01 |
| 65 | 7.278E+02 | 7.305E+02 | 3.724E-01 | 7.125E+02 | -2.102E+00 | 7.296E+02 | 2.446E-01 |
| 66 | 8.367E+02 | 8.394E+02 | 3.227E-01 | 8.118E+02 | -2.978E+00 | 8.382E+02 | 1.778E-01 |
| 67 | 1.001E+03 | 1.007E+03 | 6.432E-01 | 9.705E+02 | -3.012E+00 | 1.005E+03 | 4.538E-01 |
| 68 | 1.303E+03 | 1.317E+03 | 1.058E+00 | 1.262E+03 | -3.164E+00 | 1.312E+03 | 6.834E-01 |
| 69 | 2.180E+03 | 2.196E+03 | 7.494E-01 | 1.899E+03 | -1.289E+01 | 2.190E+03 | 4.567E-01 |

Table 6: Group constants to be evaluated:

- general data for each material: atomic weight, atomic number, fission product data and others.
- $\sigma_p$ -potential scattering cross section
- $\xi \sigma_s / \tau$ - lethargy weighted slowing down power
  where $\xi$ -average lethargy increment
  $\sigma_s$ -scattering cross-section
  $\tau$ -lethargy width
- $\sigma_{tr}$ - transport cross-section
- $\sigma_a$ - absorption cross-section
- $\nu \sigma_f$ - fission yield, where
  $\nu$ -average number of neutrons per fission
- $\sigma_f$ - fission cross-section
- $\lambda$ - Goldstein-Cohen parameter
- $\sigma_{i,j}$ - neutron scattering matrix
- $RI/\tau$ - resonance integral over a group defined as

$$RI = \int_{E_{i+1}}^{E_i} \sigma_x \, \phi \, dE$$

where $\sigma_x$ = absorption or fission yield
$\phi$ = resonance screened flux
$E_i$ = energy boundary of a group

Figure captions:

Fig. 1 Comparison of the group averaged effective fission cross-section for U-235 from the KEDAK-3 (1975) and KEDAK-3 (1979) evaluations.

Fig. 2 Comparison of the group averaged effective fission cross-section for U-235 from the ENDF/B-4 and ENDF/B-5 evaluations.

Fig. 3 Comparison of the group averaged effective fission cross-section for U-235 from the ENDF/B-5 and KEDAK-3 (1979) evaluations.

Fig. 4 Comparison of the group averaged effective fission cross-section for U-235 from the KEDAK-3 (1979) evaluation and the WIMS-D library data.

Fig. 5 Comparison of the group averaged effective fission cross-section for U-235 from the ENDF/B-5 evaluation and the WIMS-D library data.

Fig. 6 Comparison of the group averaged absorption cross-section for U-238 from the KEDAK-3 (1975) and KEDAK-3 (1979) evaluations.

Fig. 7 Comparison of the group averaged absorption cross-section for U-238 from the ENDF/B-4 and ENDF/B-5 evaluations.

Fig. 8 Comparison of the group averaged absorption cross-section for U-238 from the ENDF/B-5 and KEDAK-3 (1979) evaluations.

Fig. 9 Comparison of the group averaged absorption cross-section for U-238 from the KEDAK-3 (1979) evaluation and the WIMS-D library data.

Fig. 10 Comparison of the group averaged absorption cross-section for U-238 from the ENDF/B-5 evaluation and the WIMS-D library data.

Fig. 11 Comparison of the group averaged scattering cross-section for hydrogen bound in water at 600 K from the ENDF/B evaluation calculated according to the Haywood model and the WIMS-D library data calculated according to the effective width model.

Fig. 12 Comparison of the thermal neutron flux distribution for a chosen radial cross-section through the core of the NPP Krško as calculated by S-WIMS using the original WIMS-D data library and the ammended library with the data for U-235, U-238 and H-1 calculated from ENDF/B V.

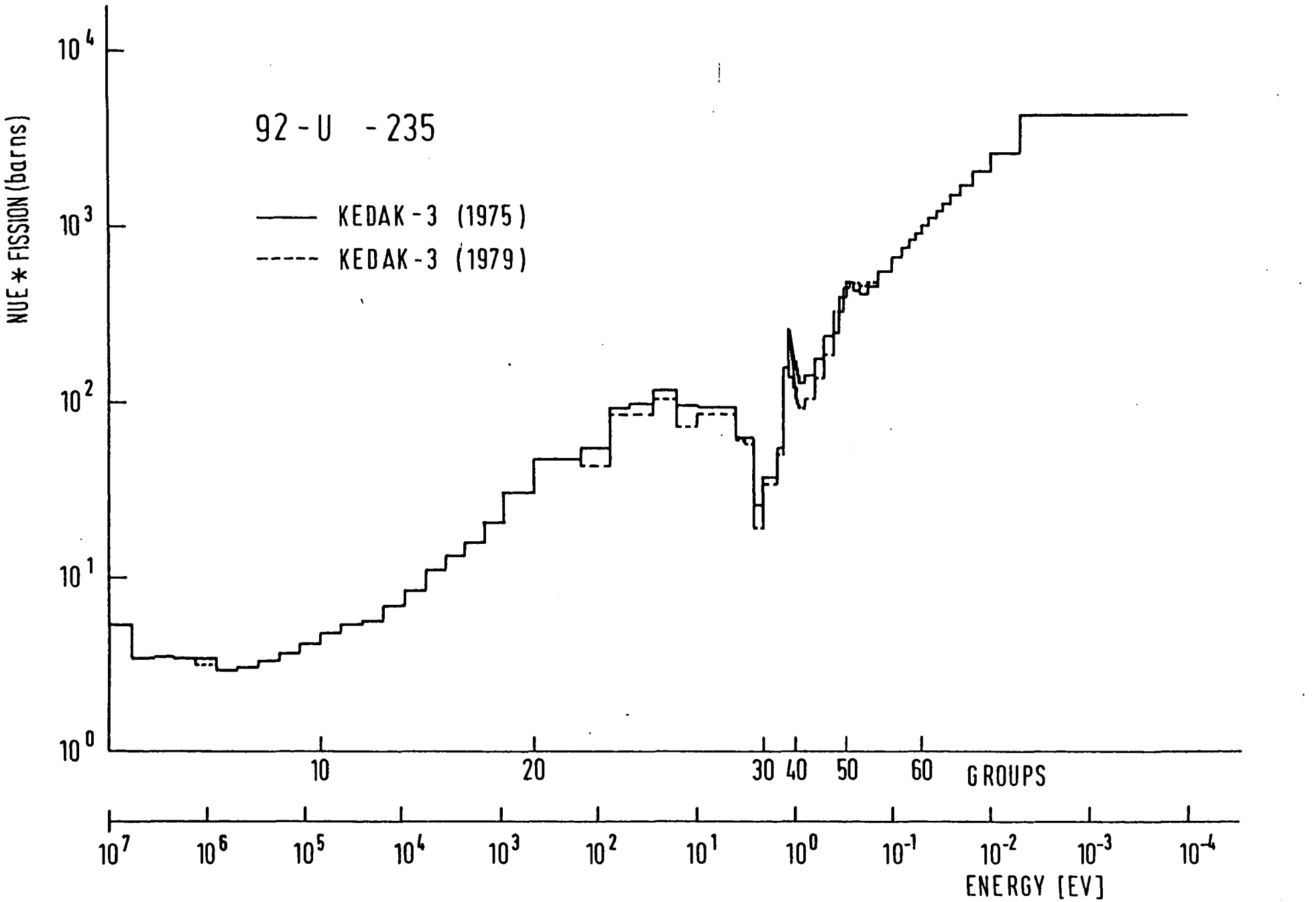
92 - U - 235
KEDAK - 3 (1975)
KEDAK - 3 (1979)
NUE * FISSION (barns)
$10^4$
$10^3$
$10^2$
$10^1$
$10^0$
10
20
30
40
50
60
GROUPS
$10^7$
$10^6$
$10^5$
$10^4$
$10^3$
$10^2$
$10^1$
$10^0$
$10^{-1}$
$10^{-2}$
$10^{-3}$
$10^{-4}$
ENERGY [EV]

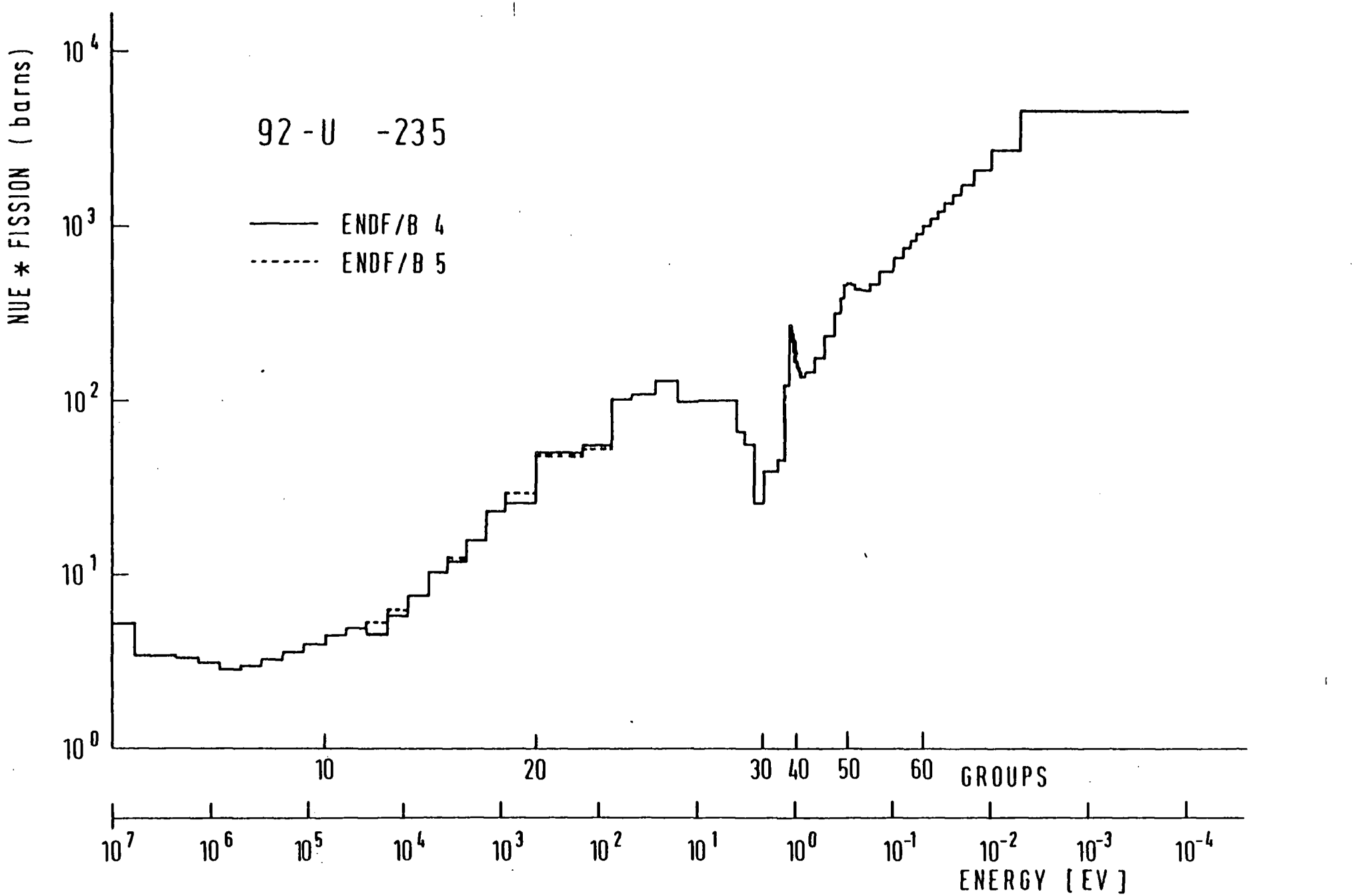
92 - U -235
ENDF/B 4
ENDF/B 5
NUE * FISSION ( barns )
$10^4$
$10^3$
$10^2$
$10^1$
$10^0$
10
20
30
40
50
60
GROUPS
$10^7$
$10^6$
$10^5$
$10^4$
$10^3$
$10^2$
$10^1$
$10^0$
$10^{-1}$
$10^{-2}$
$10^{-3}$
$10^{-4}$
ENERGY [ EV ]

Fig. 7

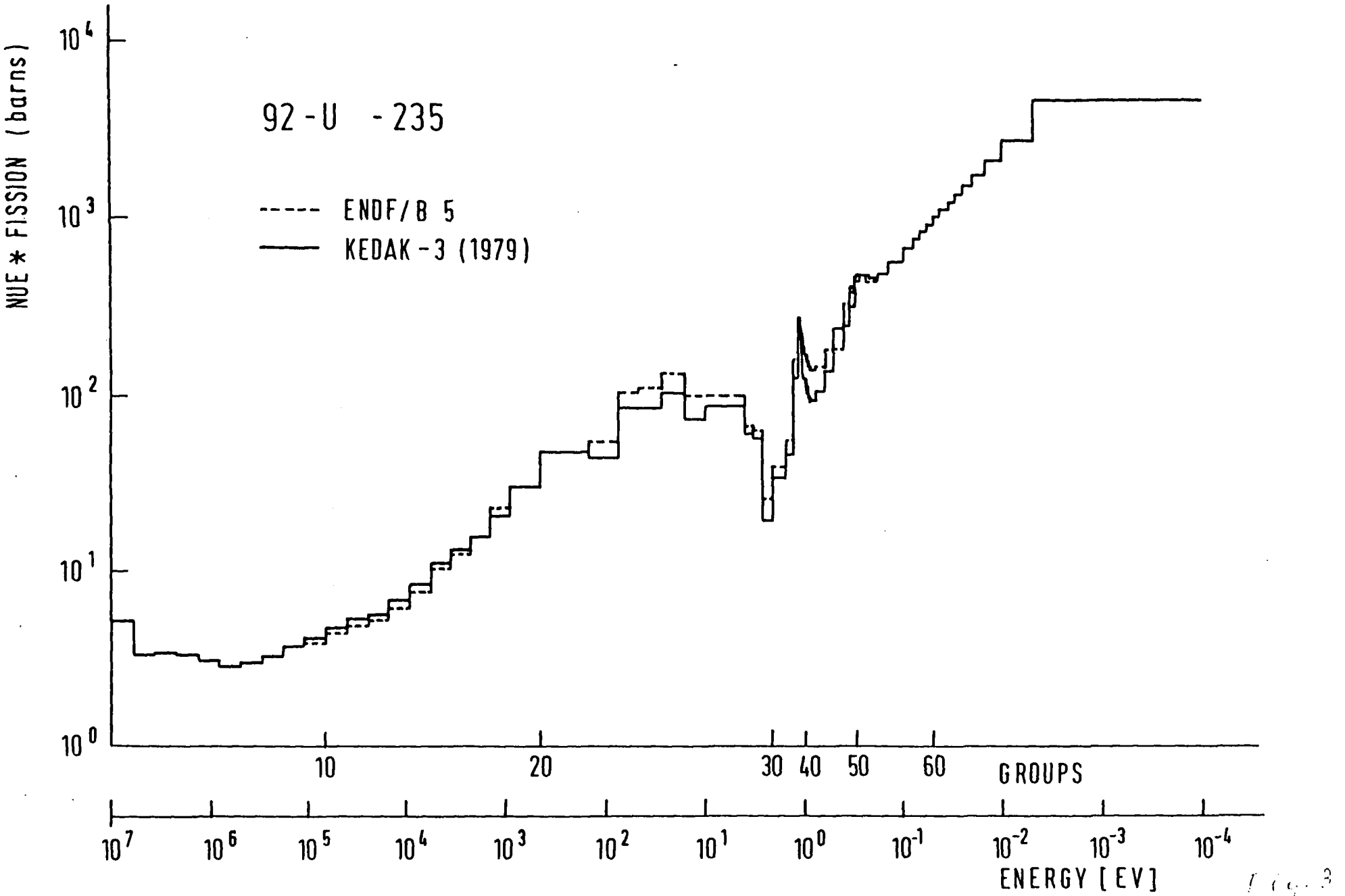
92 - U - 235
----- ENDF/B 5
——— KEDAK - 3 (1979)
NUE * FISSION (barns)
$10^4$
$10^3$
$10^2$
$10^1$
$10^0$
10
20
30 40 50 60
GROUPS
$10^7$ $10^6$ $10^5$ $10^4$ $10^3$ $10^2$ $10^1$ $10^0$ $10^{-1}$ $10^{-2}$ $10^{-3}$ $10^{-4}$
ENERGY [EV]

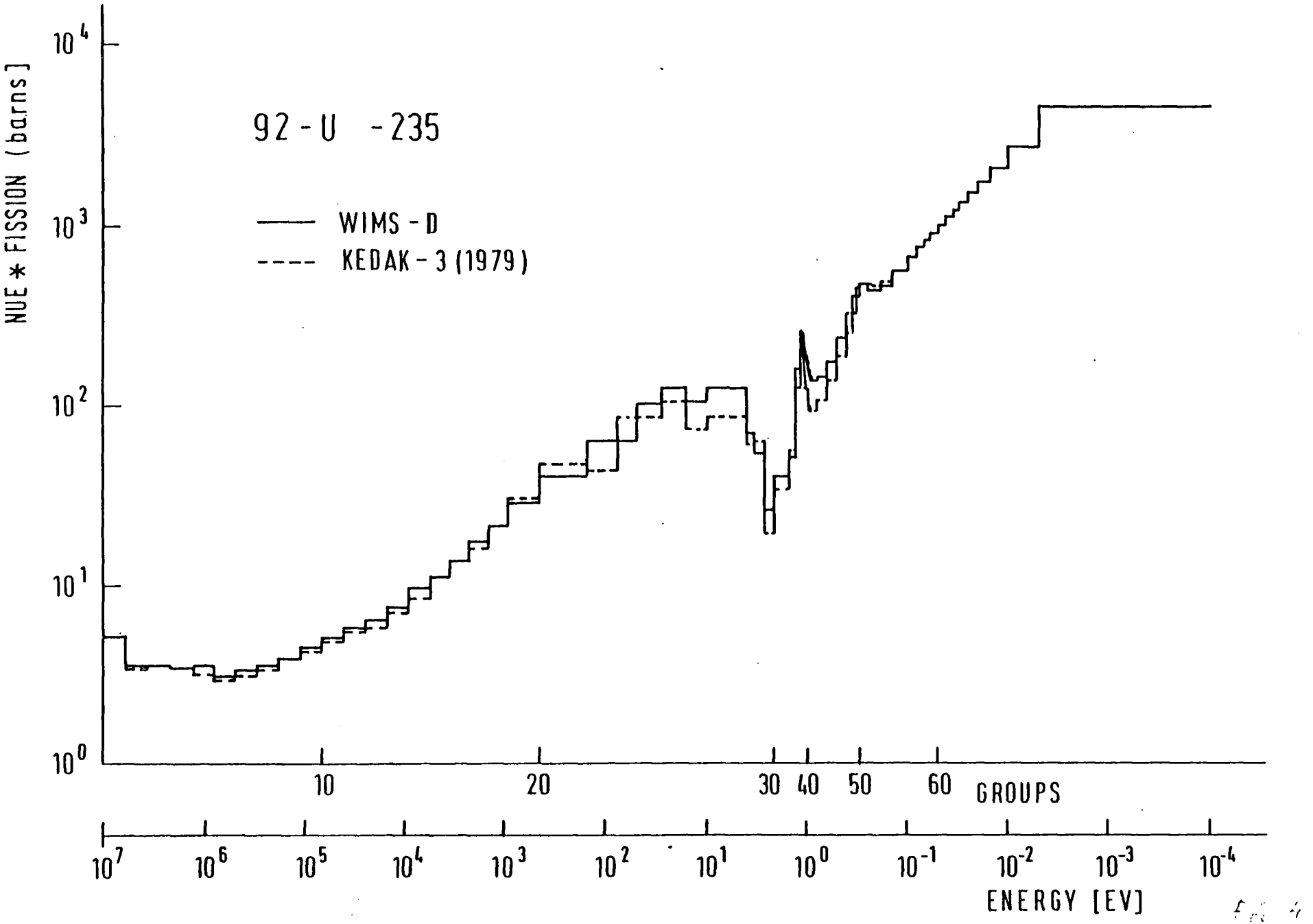
92 - U - 235
WIMS - D
KEDAK - 3 (1979)
NUE * FISSION (barns)
$10^4$
$10^3$
$10^2$
$10^1$
$10^0$
10
20
30
40
50
60
GROUPS
$10^7$
$10^6$
$10^5$
$10^4$
$10^3$
$10^2$
$10^1$
$10^0$
$10^{-1}$
$10^{-2}$
$10^{-3}$
$10^{-4}$
ENERGY [EV]

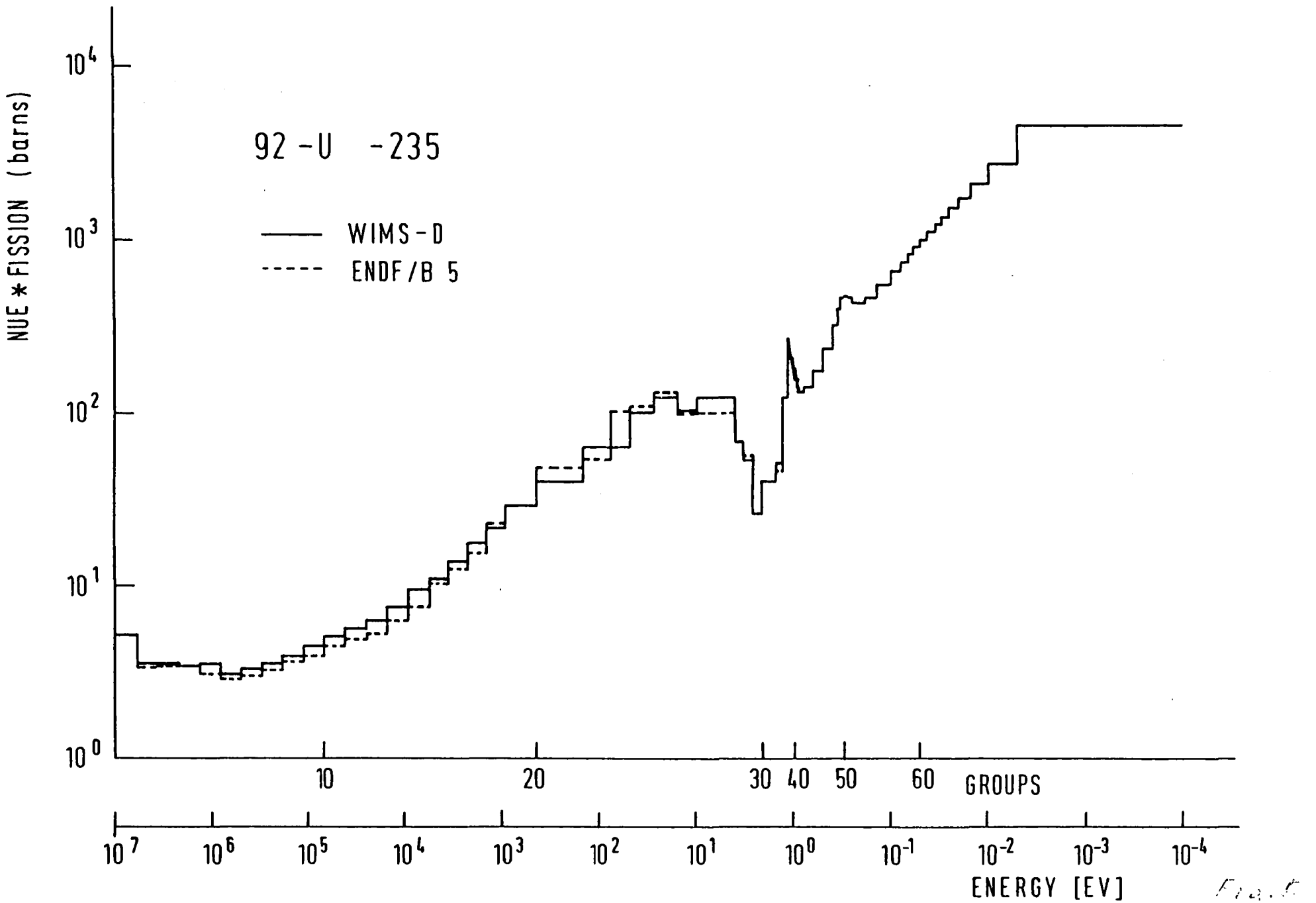
92 -U -235
WIMS - D
ENDF/B 5
NUE * FISSION (barns)
$10^4$
$10^3$
$10^2$
$10^1$
$10^0$
10
20
30
40
50
60
GROUPS
$10^7$
$10^6$
$10^5$
$10^4$
$10^3$
$10^2$
$10^1$
$10^0$
$10^{-1}$
$10^{-2}$
$10^{-3}$
$10^{-4}$
ENERGY [EV]

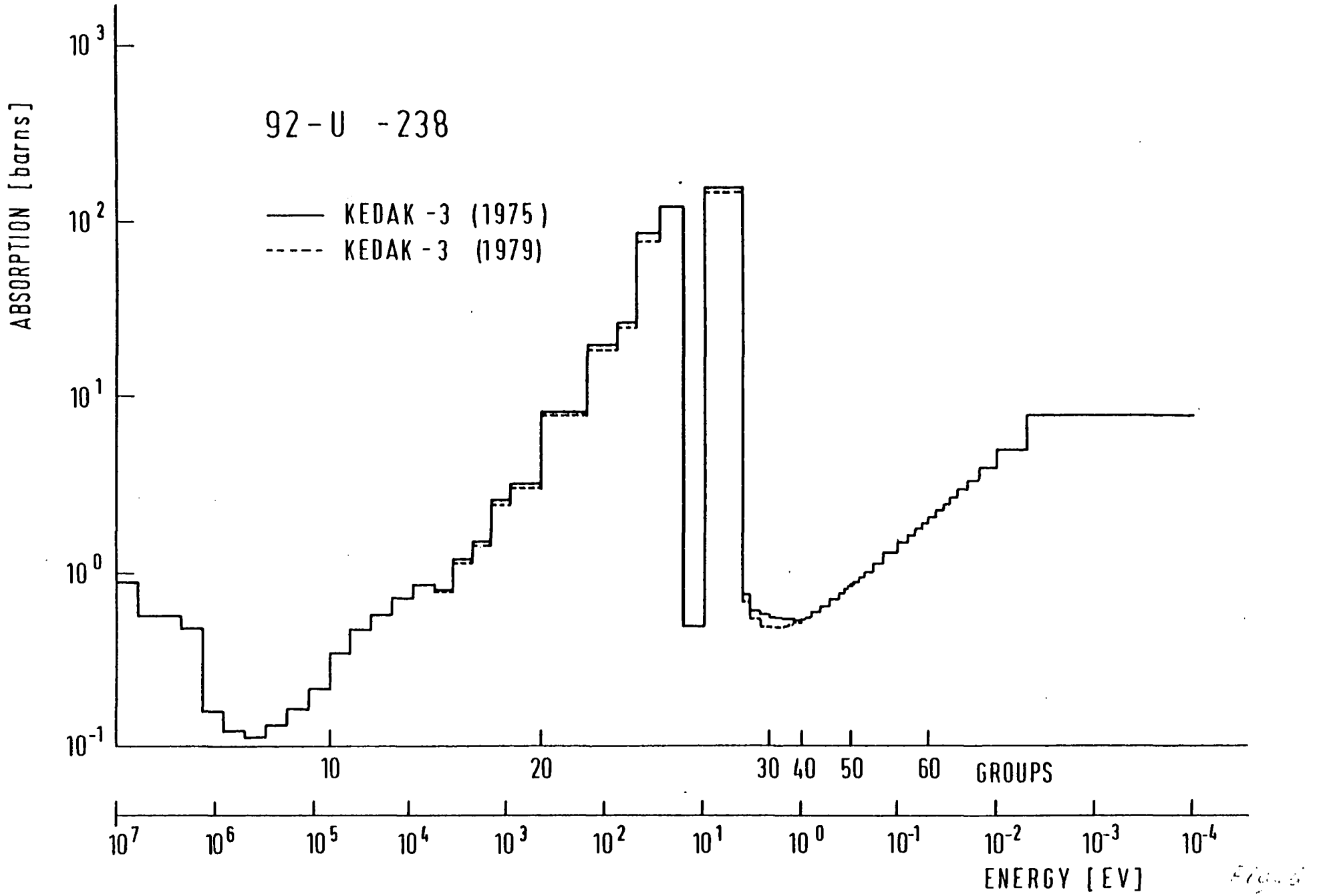
92-U -238
KEDAK -3 (1975)
KEDAK -3 (1979)
ABSORPTION [barns]
$10^3$
$10^2$
$10^1$
$10^0$
$10^{-1}$
10
20
30
40
50
60
GROUPS
$10^7$
$10^6$
$10^5$
$10^4$
$10^3$
$10^2$
$10^1$
$10^0$
$10^{-1}$
$10^{-2}$
$10^{-3}$
$10^{-4}$
ENERGY [EV]

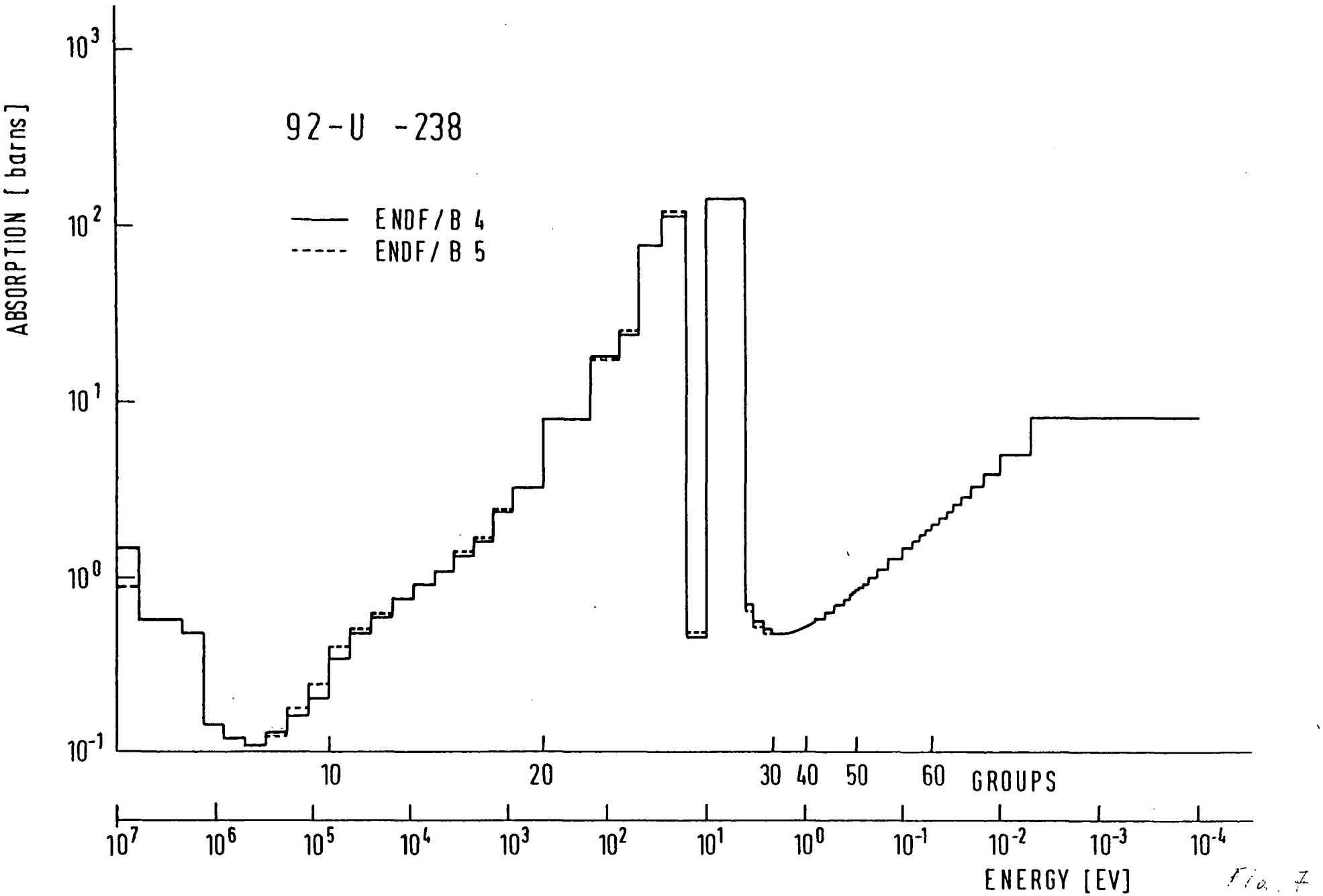
92-U -238
ENDF/B 4
ENDF/B 5
ABSORPTION [barns]
$10^3$
$10^2$
$10^1$
$10^0$
$10^{-1}$
10
20
30
40
50
60
GROUPS
$10^7$
$10^6$
$10^5$
$10^4$
$10^3$
$10^2$
$10^1$
$10^0$
$10^{-1}$
$10^{-2}$
$10^{-3}$
$10^{-4}$
ENERGY [EV]

Fig. 7

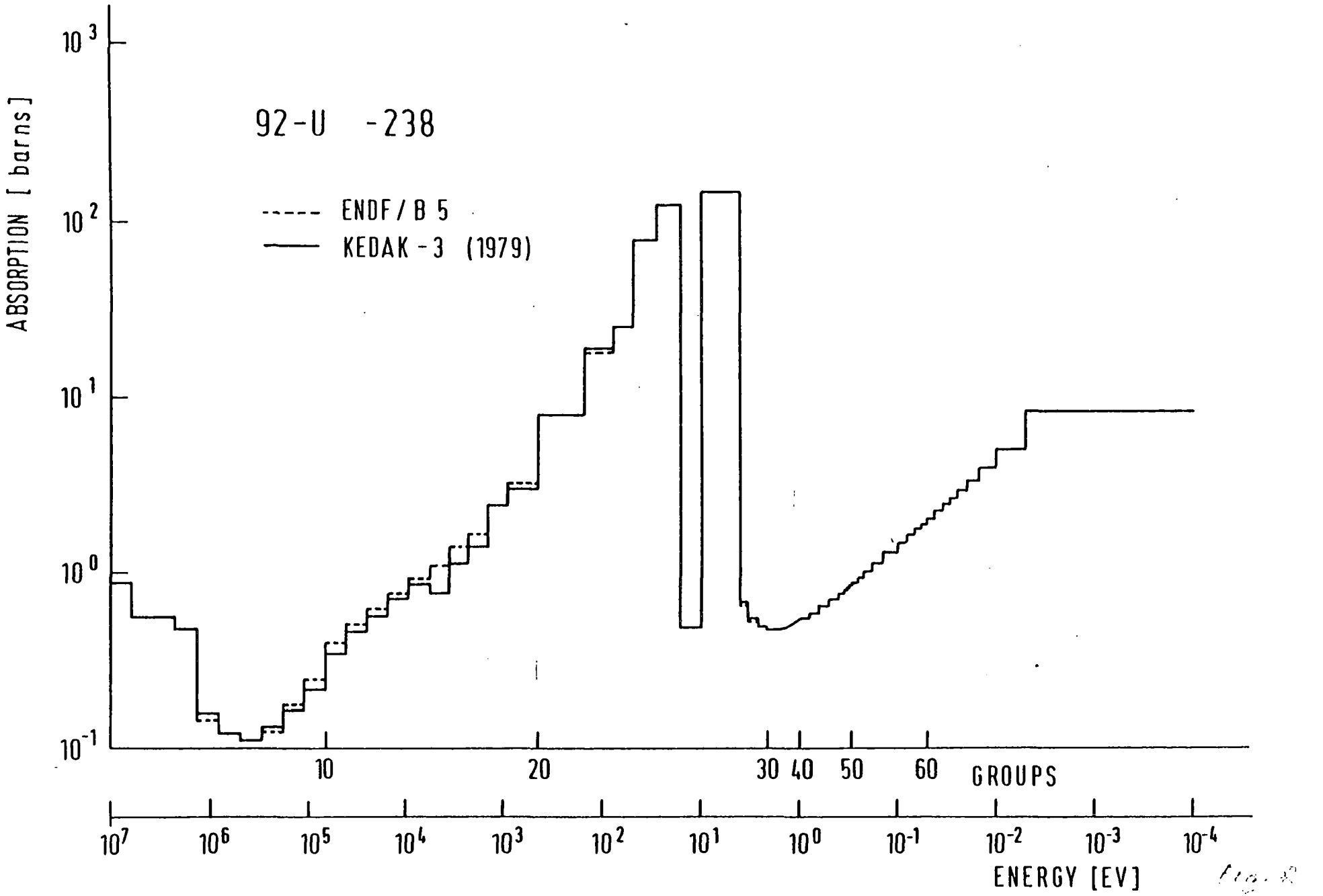
92-U -238
ENDF/B 5
KEDAK-3 (1979)
ABSORPTION [ barns ]
$10^3$
$10^2$
$10^1$
$10^0$
$10^{-1}$
10
20
30 40 50 60
GROUPS
$10^7$ $10^6$ $10^5$ $10^4$ $10^3$ $10^2$ $10^1$ $10^0$ $10^{-1}$ $10^{-2}$ $10^{-3}$ $10^{-4}$
ENERGY [EV]

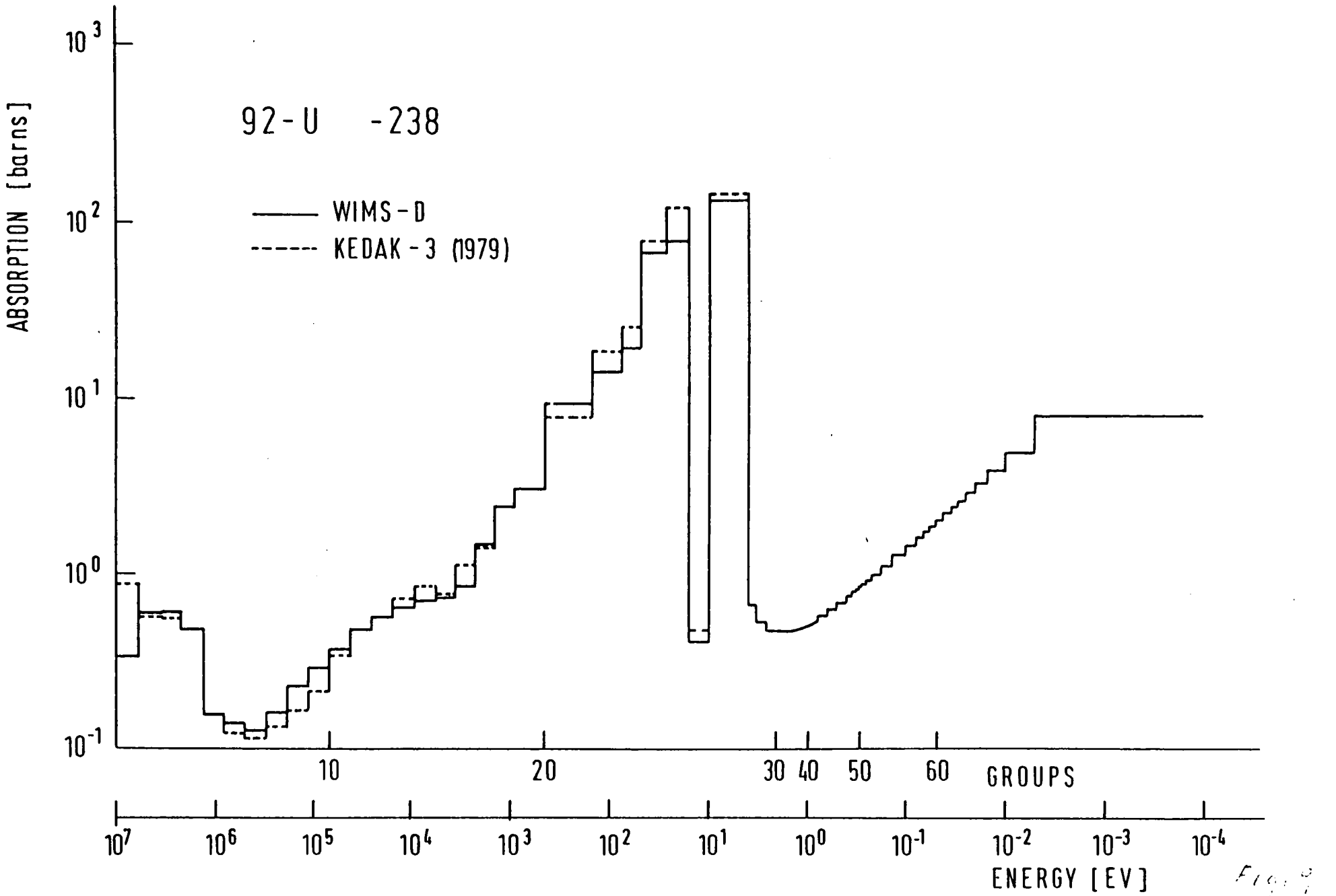
92-U -238
WIMS-D
KEDAK-3 (1979)
ABSORPTION [barns]
$10^3$
$10^2$
$10^1$
$10^0$
$10^{-1}$
10
20
30
40
50
60
GROUPS
$10^7$
$10^6$
$10^5$
$10^4$
$10^3$
$10^2$
$10^1$
$10^0$
$10^{-1}$
$10^{-2}$
$10^{-3}$
$10^{-4}$
ENERGY [EV]

Fig. 9

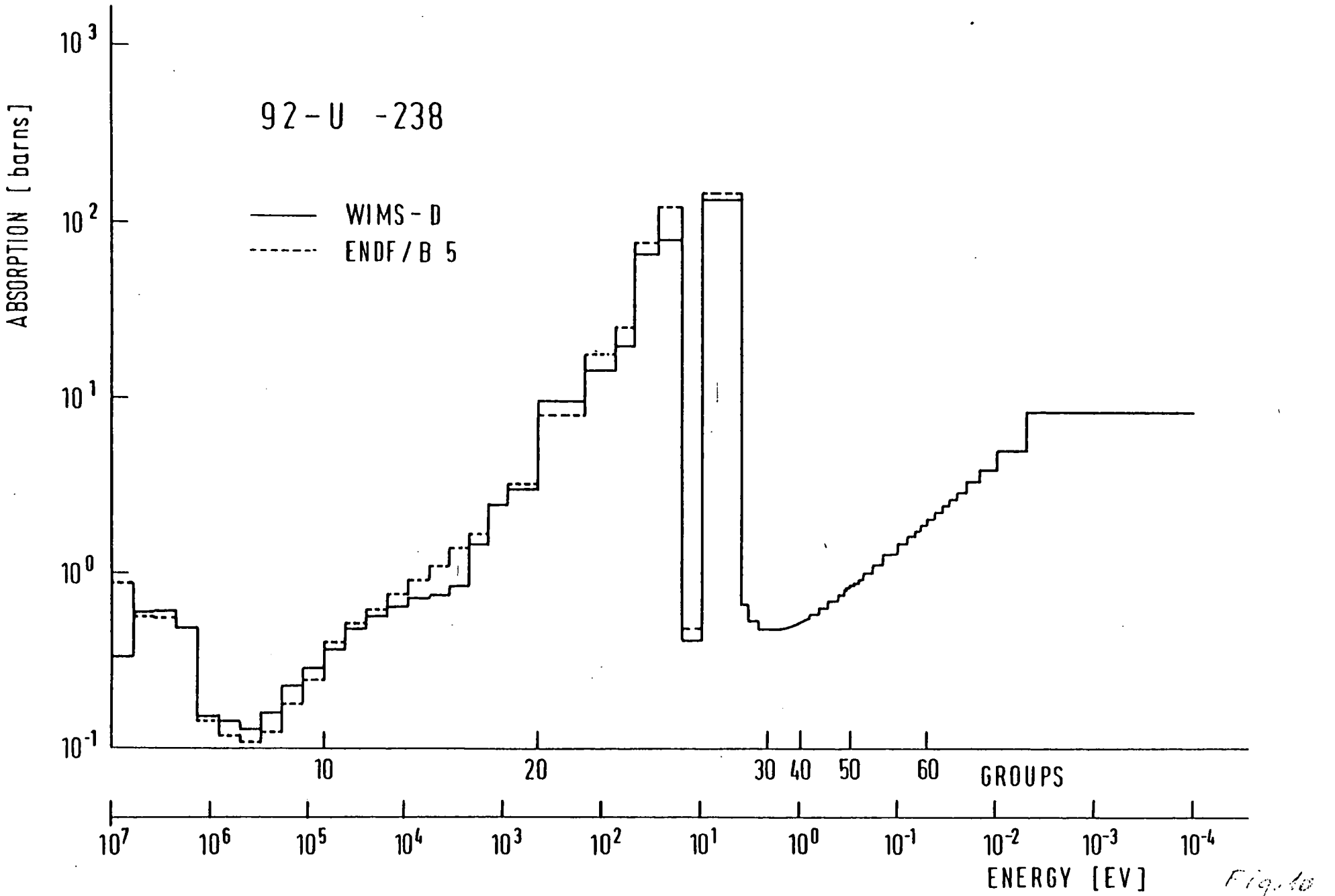
92-U -238
WIMS-D
ENDF/B 5
ABSORPTION [barns]
$10^3$
$10^2$
$10^1$
$10^0$
$10^{-1}$
10
20
30
40
50
60
GROUPS
$10^7$
$10^6$
$10^5$
$10^4$
$10^3$
$10^2$
$10^1$
$10^0$
$10^{-1}$
$10^{-2}$
$10^{-3}$
$10^{-4}$
ENERGY [EV]

Fig. 1a

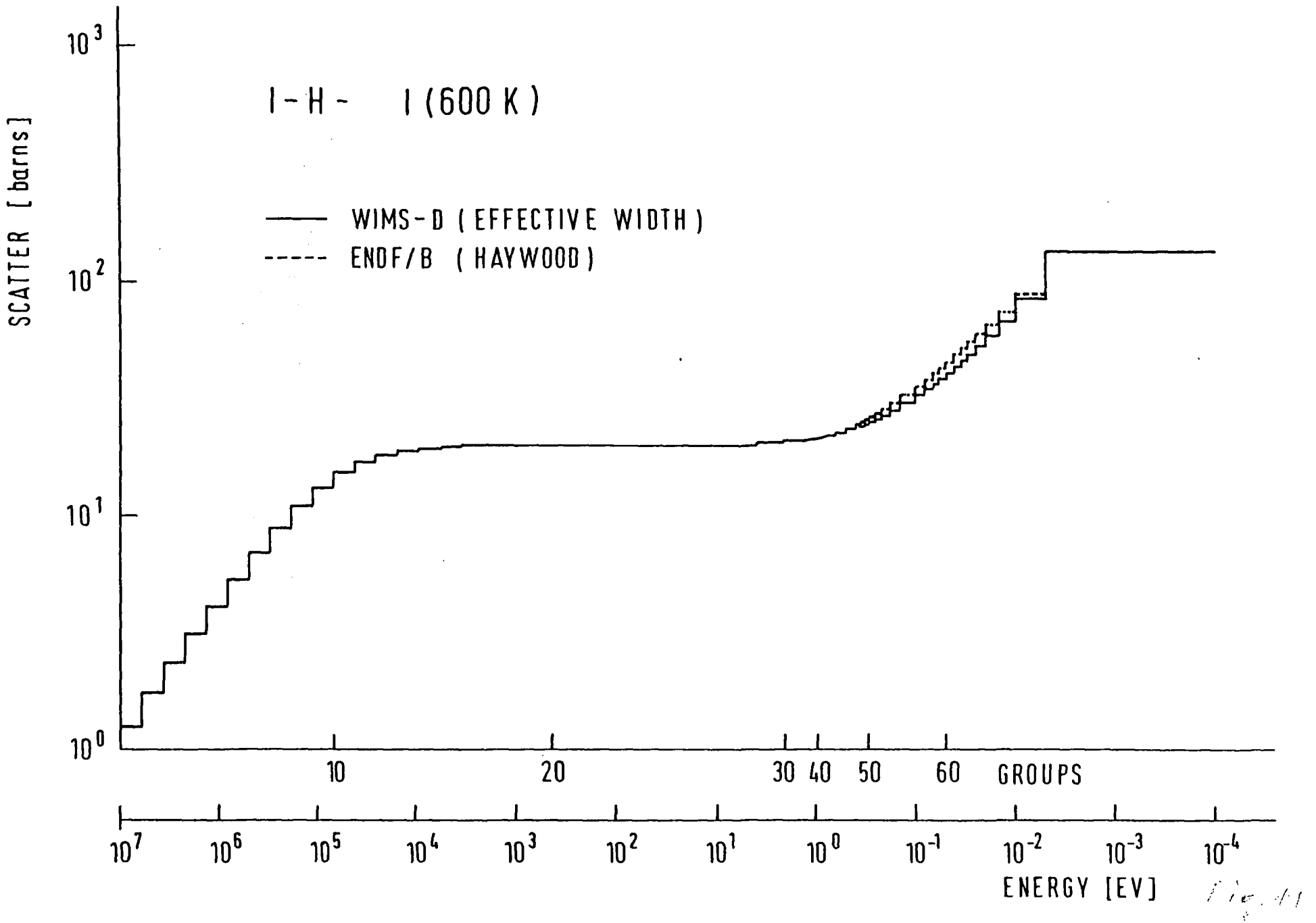
I-H- I (600 K)
WIMS-D (EFFECTIVE WIDTH)
ENDF/B (HAYWOOD)
SCATTER [barns]
$10^3$
$10^2$
$10^1$
$10^0$
10
20
30 40 50 60 GROUPS
$10^7$ $10^6$ $10^5$ $10^4$ $10^3$ $10^2$ $10^1$ $10^0$ $10^{-1}$ $10^{-2}$ $10^{-3}$ $10^{-4}$
ENERGY [EV]

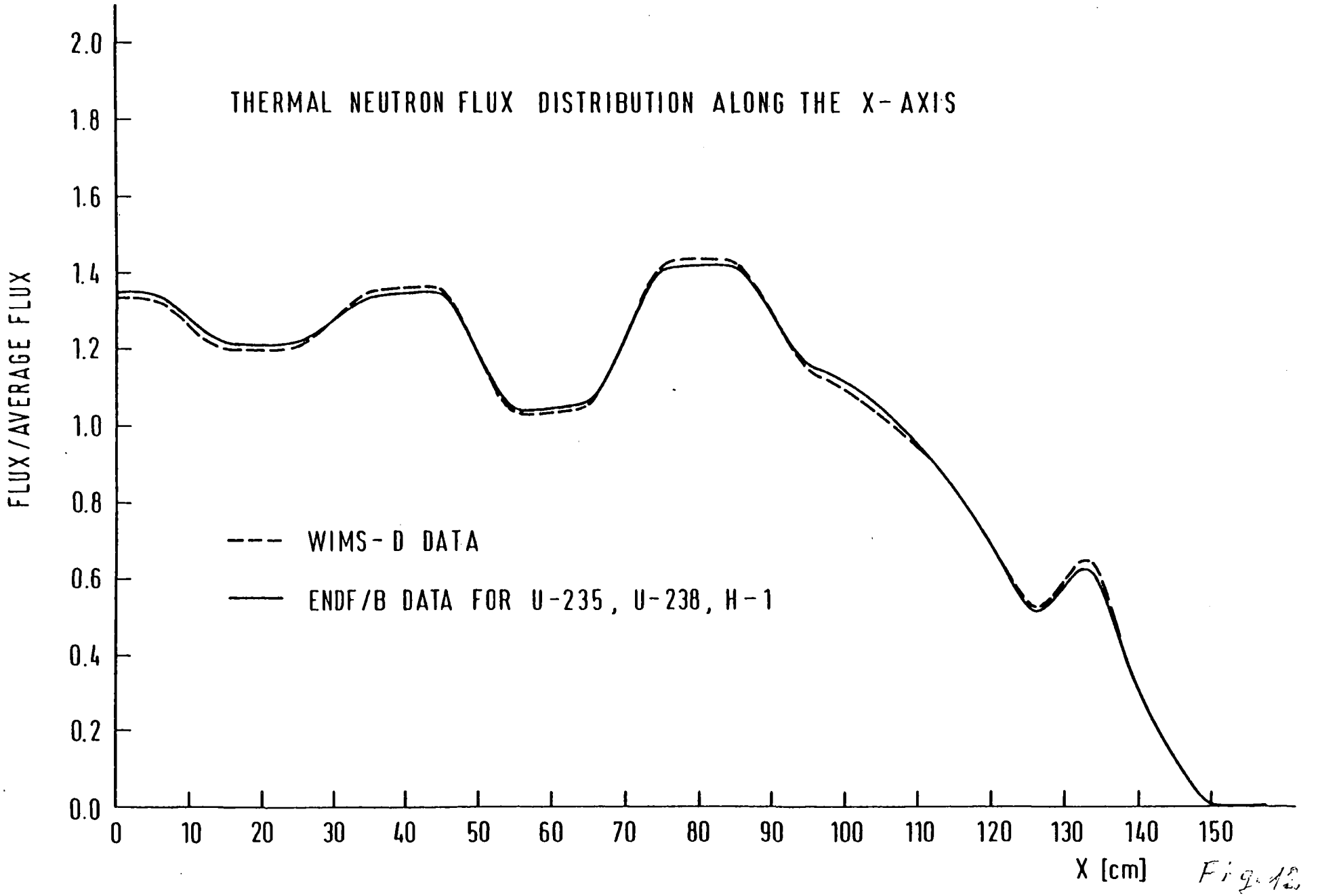
THERMAL NEUTRON FLUX DISTRIBUTION ALONG THE X-AXIS
FLUX/AVERAGE FLUX
2.0
1.8
1.6
1.4
1.2
1.0
0.8
0.6
0.4
0.2
0.0
0
10
20
30
40
50
60
70
80
90
100
110
120
130
140
150
X [cm]
--- WIMS-D DATA
—— ENDF/B DATA FOR U-235, U-238, H-1

Fig. 12